

O1 Replication Journey – Part 3: Inference-time Scaling for Medical Reasoning

Zhongzhen Huang^{1,3*} Gui Geng^{3*} Shengyi Hua^{1,3*} Zhen Huang^{4*} Haoyang Zou^{4*}
Shaoting Zhang^{1†} Pengfei Liu^{1,2,4†} Xiaofan Zhang^{1,3†}

¹Shanghai Jiao Tong University, ²SII,

³SPiRAL Lab, ⁴Generative AI Research Lab (GAIR),

Abstract

Building upon our previous investigations of O1 replication (Part 1: Journey Learning (Qin et al., 2024) and Part 2: Distillation (Huang et al., 2024)), this work explores the potential of inference-time scaling in large language models (LLMs) for medical reasoning tasks, ranging from diagnostic decision-making to treatment planning. Through extensive experiments on medical benchmarks of varying complexity (MedQA, Medbullets, and JAMA Clinical Challenges), our investigation reveals several key insights: (1) Increasing inference time does lead to improved performance. With a modest training set of 500 samples, our model yields substantial performance improvements of 6%-11%. (2) Task complexity directly correlates with the required length of reasoning chains, confirming the necessity of extended thought processes for challenging problems; (3) The differential diagnoses generated by our model adhere to the principles of the hypothetico-deductive method, producing a list of potential conditions that may explain a patient’s symptoms and systematically narrowing these possibilities by evaluating the evidence. These findings demonstrate the promising synergy between inference-time scaling and journey learning in advancing LLMs’ real-world clinical reasoning capabilities. Resources are available at <https://github.com/SPiRAL-MED/Ophiuchus>, which is a part of O1 Journey Project.

arXiv:2501.06458v1 [cs.CL] 11 Jan 2025

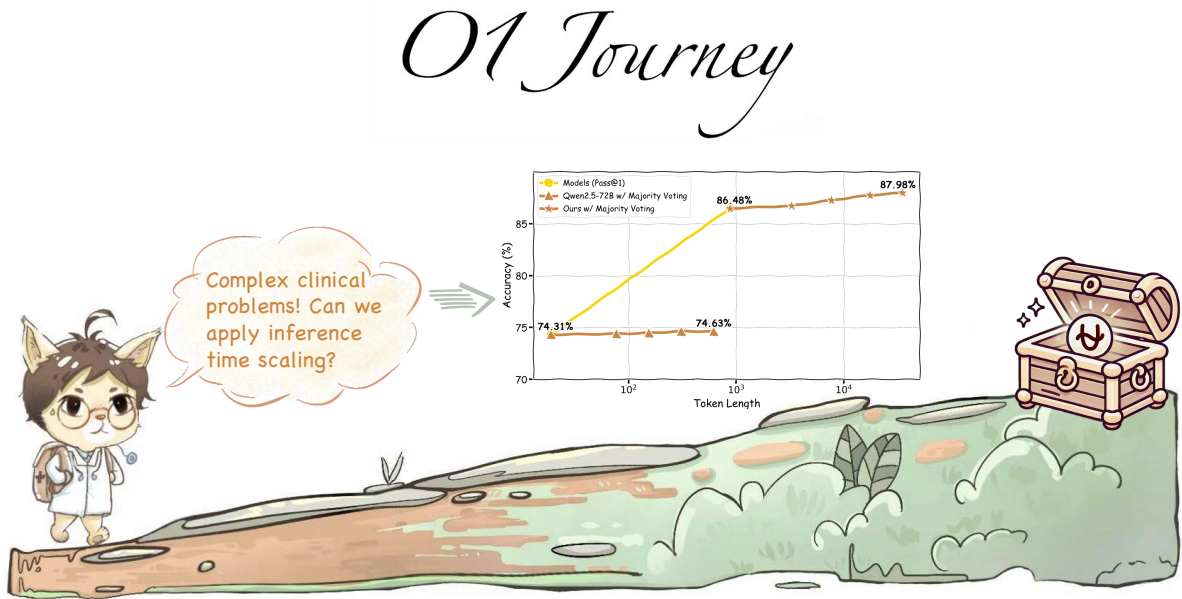


Figure 1: Illustration of our O1 replication journey in the medical field. which aims to develop systems capable of deep scientific thinking, ultimately enabling AI-driven breakthroughs in medical domains.

* Co-first authors

† Corresponding author

1 Introduction

Medicine is an endeavor that fundamentally involves complex reasoning, spanning tasks from diagnostic decision-making to treatment planning. Intricate reasoning is particularly crucial in medical scenarios where patient outcomes depend on understanding multifactorial conditions (Singhal et al., 2023; Qiu et al., 2024). The process of differential diagnosis (Seller and Symons, 2011) exemplifies this complexity, requiring physicians to generate a list of potential diagnoses and methodically narrow it down by evaluating clinical findings and excluding options that do not align with the evidence. This process demands not only deep clinical knowledge but also the ability to draw logical inferences and evaluate multiple hypotheses based on available evidence. In recent years, the emergence of large language models (LLMs) holds significant promise for advancing clinical applications. However, the complexity of medical reasoning poses unique challenges that traditional scaling methods—such as increasing model parameters or training data volume (Kaplan et al., 2020; Brown et al., 2020; Chowdhery et al., 2023)—struggle to address effectively. Recent studies (Snell et al., 2024; OpenAI, 2024) have demonstrated that scaling inference time can lead to more efficient improvements in LLM performance. This approach, known as *inference-time scaling*, allows more processing time for complex tasks, enabling step-by-step problem-solving and iterative refinement of the reasoning process. OpenAI’s O1 (OpenAI, 2024) particularly emphasizes this strategy by scaling inference time to generate long thoughts for complex reasoning.

While previous studies (Huang et al., 2024; Jiang et al., 2024; Zhang et al., 2024a,b; Kimi, 2024; o1 Team, 2024; Team, 2024b) have validated inference-time scaling in various domains such as mathematical reasoning, its application to medical scenarios presents unique opportunities and challenges. Building on our previous work on journey learning (Qin et al., 2024), we posit that complex clinical scenarios—requiring integration of established knowledge with nuanced patient histories and comorbidities—necessitate even longer reasoning processes. Our initial explorations demonstrated significant improvements (Figure 1) when scaling inference time to account for multiple clinical factors and iteratively refine diagnostic strategies. This work examines how LLMs with *inference-time scaling* adapt to varying task complexities in medicine, focusing on two key aspects: (1) identifying optimal scenarios for assessing performance variations with *inference-time computing*, and (2) developing effective methods to synthesize supervised fine-tuning data for generating extended reasoning chains. To validate our approach, we utilize public medical benchmarks proposed by (Chen et al., 2024), encompassing challenging clinical cases and medical licensing examinations. A key challenge lies in enabling effective journey learning during inference. Building on previous work (Huang et al., 2024), we employ a straightforward yet effective knowledge distillation approach (Hinton, 2015) from GPT-series models. Key findings from our experiments include the following: (1) majority voting provides a straightforward approach to augment inference-time computation, though its effectiveness is constrained in complex scenarios; (2) effective scaling of inference time, however, depends on the sufficient capacity of LLMs, otherwise, such efforts are likely to be in vain; (3) tasks with greater complexity necessitate longer reasoning processes, reinforcing the need for extended thought chains as task difficulty increases; and (4) removing multiple-choice options and encouraging free-form responses unlocks the potential for medical journey learning, fostering nuanced clinical reasoning.

Looking ahead, the integration of *inference-time scaling* into clinical applications presents both opportunities and challenges. Our work underscores the potential of this approach to address complex medical tasks, but it also highlights the need for continued exploration and innovation. By releasing key findings, distilled datasets, and experimental methodologies, we aim to contribute to the broader AI research community and foster collaborative advancements. Furthermore, we advocate for a research ethos rooted in transparency, originality, and rigorous evaluation, particularly as AI systems become more deeply embedded in critical domains like healthcare. While the distillation strategy and its implications warrant further scrutiny, we hope this study catalyzes future investigations into *inference-time scaling* and its capacity to enhance the reasoning capabilities of LLMs. Ultimately, our goal is to inspire new methodologies and applications that bridge the gap between computational innovation and practical medical impact, ensuring better outcomes for patients and practitioners alike.

2 Exploration Process

The conclusion derived from analyzing examples provided by OpenAI ¹ demonstrates that **as the difficulty increases, the inference time tends to grow proportionally** (Qin et al., 2024). This suggests that higher-difficulty problems require more reasoning steps, which in turn necessitate a longer inference time. Although the exact mechanisms through which *inference-time scaling* enhances problem-solving remain underexplored, it is evident that *inference-time scaling* contributes significantly to identifying and analyzing key information. This phenomenon is particularly critical in medical domains, where clinicians require much time to process data from multiple sources and modalities when diagnosing conditions, making prognostic evaluations, and determining treatment plans. In

¹<https://openai.com/index/learning-to-reason-with-llms>

the following parts, we document our exploration of evaluating the utility of *inference-time scaling* in addressing complex, domain-specific challenges in medicine.

2.1 Benchmark Overview

To demonstrate the effectiveness of *inference-time scaling* in addressing medical problems, we selected three benchmarks in (Chen et al., 2024) for our experiments: the JAMA Clinical Challenge (JAMA), Medbullets, and MedQA. These benchmarks encompass challenging real-world clinical cases from various medical domains as well as medical licensing exams of different difficulty levels. The JAMA dataset includes 1,524 examples collected from the JAMA Network Clinical Challenge² archive, spanning the past decade (July 2013–October 2023) and covering 13 medical domains. The examples are based on complicated clinical scenarios involving patient history, family history, laboratory results, physical/radiology/cardiology analysis, etc., and hence require more sophisticated understanding and reasoning to “arrive at a correct diagnosis”. At this stage, our primary goal is to examine the effectiveness of *inference-time scaling* on complex tasks. Therefore, we focused on cases that o1-mini struggles with. Specifically, we utilized a streamlined subset of JAMA containing 646 cases, half of which are challenging for o1-mini, for evaluation.

The Medbullets and MedQA datasets in use are based on the National Medical Board Examination in the United States or the United States Medical Licensing Examination (USMLE). Medbullets is an online platform that provides medical study resources. The dataset focuses on Medbullets *Step 2/3*³ which serves USMLE *Step 2&3*⁴ type questions. The resolution of the questions in *Step 2/3* demands the application of medical knowledge and clinical reasoning rather than relying solely on textbook knowledge (*Step 1* questions). The dataset consists of 308 examples posted on the X (formerly Twitter)⁵ platform between April 2022 and December 2023. Each comprises a case description, a question, five answer choices, and an explanation that explains each option. MedQA also includes questions from the Medbullets website but without the aforementioned explanations. The test set includes 679 *Step 1*⁶ questions and 594 *Step 2/3* questions, obtained in March 2021, ensuring that there is no overlap with the Medbullets dataset. The involvement of these two datasets provides insights into whether *inference-time scaling* helps or hinders tackling medical tasks of various difficulty levels, and how it takes effect.

2.2 Journey Learning Data Synthesis

To enable LLMs to perform journey learning during the problem-solving process, we need to construct a collection of high-quality demonstration data that exhibits this behavior. Building on prior efforts, we adopted a distillation-based approach for producing high-quality data. In the era of LLMs, instructing weaker models using stronger ones is common practice for advancing models. Recent research (Taori et al., 2023; Xu et al., 2023; Gunasekar et al., 2023) highlights that fine-tuning with high-quality data synthesized from proprietary models can achieve remarkable outcomes. In our exploration, we utilized o1 to collect journey learning data, synthesizing two types of long-form data: LongStep and LongMonolog.

LongStep: Upon analyzing responses from o1 and GPT-4o, we observed that o1 generates longer solution steps that include more detailed processes for analyzing key information. Given o1’s exceptional performance and sophisticated reasoning capabilities, we extracted its solution steps to train LLMs to emulate this behavior, producing more thorough and detailed solutions.

LongMonolog: In practice, the examples provided by OpenAI often exhibit a relatively flexible, sometimes colloquial, “inner monolog” style. However, the internal thought processes of o1 cannot be directly accessed because it summarizes these processes before presenting them to the user. Despite this, its summarized internal thoughts are still valuable, as they outline the key stages of problem-solving. That said, the summarized thoughts are not directly suitable for training. Inspired by (Huang et al., 2024), we designed prompts to instruct o1-preview to expand its summarized thoughts into a long-form reasoning. Careful prompt design is essential, as o1 imposes restrictions on accessing its internal reasoning processes. The resulting output adheres to specific guidelines, ensuring that the solutions resemble an inner monologue, are highly detailed and reflective, including self-corrections, and exhibit extended reasoning. After collecting labeled data, we performed further preprocessing to ensure data quality and standardization of output formats.

At the current stage, our primary goal is to evaluate the role of *inference-time scaling* in addressing medical problems. Our objective is not to directly perform differential diagnosis, which we acknowledge as extremely difficult given the limited information and resources available. In real-world scenarios, differential diagnosis aligns with the principles of the hypothetico-deductive method, where potential diseases or conditions are treated as

²<https://jamanetwork.com/collections/44038/clinical-challenge>

³<https://step2.medbullets.com/>

⁴<https://www.usmle.org/step-exams/step-2-ck>

⁵<https://x.com/medbullets>

⁶<https://step1.medbullets.com/>

hypotheses that clinicians evaluate to determine their validity. To simplify the task, we adopt multiple-choice datasets in this section, allowing potential diagnoses (the “differential”) can be predefined to guide the model in generating hypotheses. We opt not to use in-house data, as real-world clinical scenarios often contain a substantial amount of irrelevant information that can interfere with reasoning. This poses a great challenge for current models. In contrast, public benchmarks simplify the problem and eliminate some of this interference. Moreover, the choices from MedQA and JAMA are carefully designed to be similar and plausible options. In analyzing these options to determine the final answer, the process closely mirrors the thought process involved in clinical diagnosis. Moreover, the key factor in data selection was the length of the problem-solving process. We excluded cases with a short thought process. Collectively, we assembled a training dataset consisting of 500 examples, with 350 drawn from the training set of MedQA (Jin et al., 2020) and 150 from the remaining set of the JAMA Clinical Challenge. The average length is 729 for the curate LongStep dataset and 1,223 for the LongMonolog dataset, respectively. Examples of our distilled data are presented in Figures 9, 11 and 12.

Model Name	Param. Size	Mean Acc.	JAMA (646)		Medbullets (308)		MedQA (1273)	
			Acc.	#Avg. Token	Acc.	#Avg. Token	Acc.	#Avg. Token
<i>Proprietary</i>								
GPT-4o	-	80.01	63.77	-	77.92	-	88.76	-
GPT-4o-Vanilla CoT	-	81.83	63.77	335	81.68	323	91.04	300
o1-mini	-	77.45	50.00	-	80.51	-	90.65	-
o1-preview	-	87.95	73.21	-	89.28	-	95.12	-
<i>Open Source Models</i>								
Qwen2.5	7B	51.23	42.41	-	46.75	-	56.79	-
Qwen2.5-Vanilla CoT	7B	49.61	40.40	371	46.42	353	55.06	344
InternLM2.5	7B	45.84	39.78	-	43.18	-	49.56	-
InternLM2.5-Vanilla CoT	7B	42.47	34.05	303	38.63	273	48.15	291
LLama3.1	8B	55.71	46.67	-	49.43	-	61.82	-
InternLM2.5	20B	51.90	43.34	-	49.02	-	56.95	-
InternLM2.5-Vanilla CoT	20B	51.18	42.41	312	46.01	330	56.87	323
Qwen2.5	32B	64.20	49.84	-	59.74	-	72.58	-
Qwen2.5-Vanilla CoT	32B	65.86	50.92	351	61.68	332	74.46	329
LLama3.1	70B	71.39	59.59	-	67.85	-	78.24	-
LLama3.1-Vanilla CoT	70B	73.59	57.27	529	66.55	496	83.11	477
Qwen2.5	72B	65.82	50.15	-	63.63	-	74.31	-
Qwen2.5-Vanilla CoT	72B	69.10	50.15	435	65.58	387	79.57	375
<i>Supervised Fine-tuning with Vanilla CoT</i>								
Qwen2.5-CoT SFT	32B	67.13	52.16	383	61.03	340	76.19	323
LLama3.1-CoT SFT	70B	74.48	56.03	386	72.07	342	84.44	333
Qwen2.5-CoT SFT	72B	70.94	53.09	402	67.20	355	80.91	346
<i>Ours (Journey Learning)</i>								
Qwen2.5-LongStep	32B	70.08	56.34	759	66.23	645	78.00	615
Qwen2.5-LongMonolog	32B	70.23	53.71	1098	68.50	1023	79.02	997
LLama3.1-LongStep	70B	76.59	60.21	819	74.67	721	85.38	669
LLama3.1-LongMonolog	70B	77.36	<u>59.44</u>	1153	77.27	1029	86.48	953
Qwen2.5-LongStep	72B	75.51	58.66	762	72.07	692	84.91	631
Qwen2.5-LongMonolog	72B	<u>77.18</u>	59.28	1076	<u>76.29</u>	917	86.48	873

Table 1: Performance comparison of proprietary, open-source, and supervised fine-tuned models across three medical benchmarks. The metrics include accuracy (Acc.) and average output token length (Avg. Token). Mean Acc. represents the weighted average across the three datasets. The best score excluding closed-source APIs was bolded, and the second-best score was underlined.

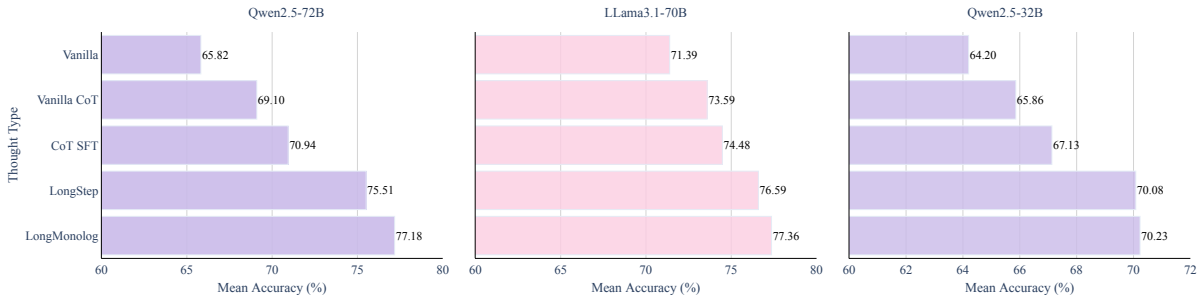


Figure 2: Weighted mean accuracy of Qwen2.5-72B-Instruct, LLama3.1-70B, and Qwen2.5-32B across three datasets using distinct strategies.

3 Experiments

3.1 Implementation Details

In our pilot studies, we found that current open-source LLMs still lag significantly behind commercial closed-source APIs. Considering resource constraints and the need to share our results with the community promptly, we selected Qwen2.5-32B-Instruct (Team, 2024a), Qwen2.5-72B-Instruct (Team, 2024a) and LLama3.1-70B-Instruct (AI@Meta, 2024) as our base models due to their foundational capabilities in medicine. This foundational knowledge ensures a solid starting point for subsequent long reasoning processes and improvements. We utilized Llama-Factory (Zheng et al., 2024) to perform instruction tuning on the LLMs with LoRA (Hu et al., 2021). Additionally, we employed DeepSpeed optimization (Rasley et al., 2020) with ZeRO-3 configuration. Following the methodology outlined in (Qin et al., 2024; Huang et al., 2024), we set the number of training epochs to three. All LLMs were fine-tuned on 8 NVIDIA A800 GPUs using a learning rate of 1×10^{-4} and a batch size of 8.

3.2 Main Results

In this study, we present a comprehensive performance comparison of various methods on the evaluation benchmarks listed in Table 1. The results include performance metrics for proprietary APIs, open-source baselines, and several models fine-tuned on our synthesized data. In Table 1, the rows with the “-Vanilla CoT” suffix indicate models or APIs that solve problems step by step using Chain-of-Thought prompts according to (Wei et al., 2022). We selected models that benefit from introducing a reasoning process (highlighted in red) for further experiments. The rows marked in orange (“-CoT SFT” suffix) show the result of models trained with vanilla CoT from GPT-4o. The rows marked in blue correspond to models, with the “-LongStep” suffix and “-LongMonolog” suffix, fine-tuned on our two journey learning datasets. Additionally, we measure the average token count of each model’s outputs via “tiktoken”.⁷ This is crucial for evaluating the effectiveness of inference time scaling schemes. The results demonstrate that these methods significantly improve model performance even with minimal training data. These findings highlight the effectiveness of inference-time computing in enhancing the complex reasoning capabilities of LLMs for addressing medical challenges. A more detailed analysis can be seen in the next sections.

3.3 Does Inference-time Scaling Help?

To intuitively illustrate the contribution of *inference-time computing*, we present the accuracy of Qwen2.5-72B, LLama3.1-70B, and Qwen2.5-32B across three datasets using distinct strategies: vanilla usage, vanilla CoT prompting, CoT SFT, long step SFT, and long monolog SFT. As shown in Figure 2, each strategy significantly improves overall accuracy. Notably, Qwen2.5-72B achieves gains of +3.28%, +5.12%, +9.69%, and +11.36% for the respective strategies, strongly supporting the hypothesis that incorporating structured thought processes in inference time enhances the ability of powerful models to address complex medical problems.

A key observation is that **more inference time leads to enhanced performance**. For instance, when Qwen2.5-72B employs step-by-step reasoning, whether via vanilla CoT or CoT fine-tuning, the output token length ranges from 300 to 500 tokens, resulting in about 5% increase in mean accuracy. In contrast, under the journey learning settings, which include long step and long monolog fine-tuning, the token count extends to approximately 1,000, yielding improvements of about 10%. A similar trend is evident for Qwen2.5-32B and LLama3.1-70B, as depicted in the remaining figures of Figure 2. Specifically, LLama3.1-70B achieves improvements of +2.20%, +3.09%, +5.20%, and +5.97%, while Qwen2.5-32B shows gains of +1.66%, +2.93%, +5.88%, and +6.03% across the three reasoning strategies.

⁷<https://github.com/openai/tiktoken>

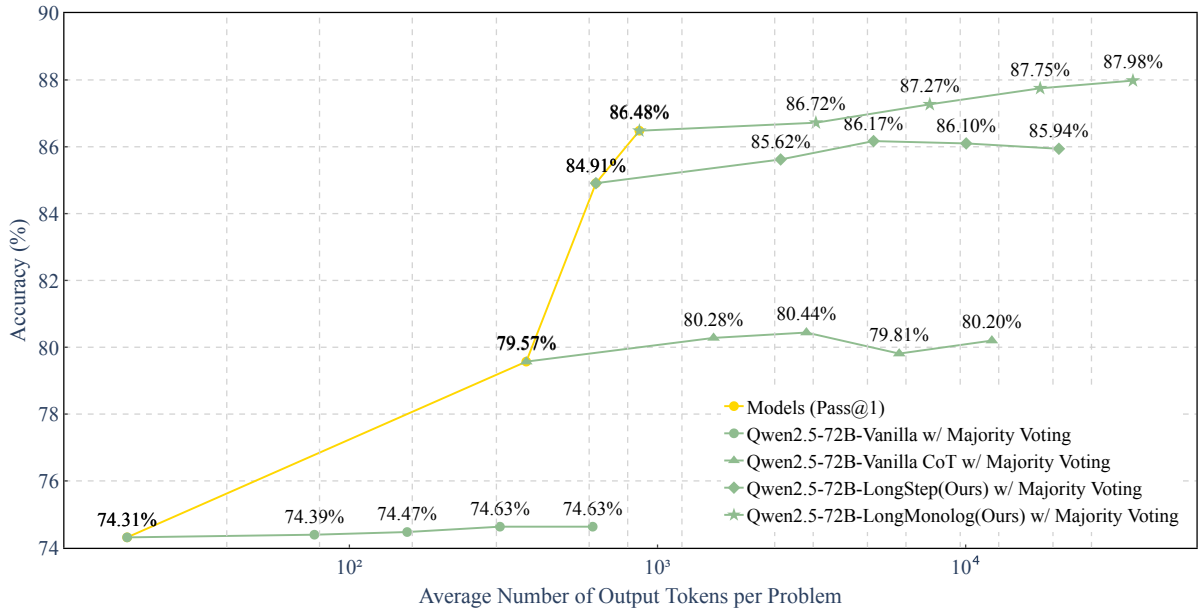


Figure 3: The Accuracy of Qwen2.5-72B-Series on MedQA with inference-time scaling.

When comparing LongStep and LongMonolog, it remains challenging to determine which consistently delivers superior performance. Based on current experimental data, long monolog demonstrates higher accuracy on Medbullets and MedQA but does not maintain its advantage in JAMA. For instance, Qwen2.5-32B achieves 56.34% accuracy in JAMA with LongStep but only 53.71% with LongMonolog. The limitation in Qwen2.5-32B’s self-reflective reasoning may stem from its inability to construct a complete thought leading to correctness. As shown in Figures 10, 13 and 14, extended steps result in correct answers, whereas redundant reflections sometimes lead to errors (red texts in Figure 14). This finding suggests an assumption that long thought processes during inference time can aid in answering complex medical questions but require sufficient domain knowledge.

How about scaling the inference time by majority voting? Majority voting is an intuitive plug-and-play approach commonly used for scaling inference time by leveraging the collective reasoning process across different computational runs. To investigate the superimposed effect of majority voting and the aforementioned schemes, we conducted experiments with the Qwen2.5-72B model on the MedQA dataset. The results, illustrated in Figure 3, compare the performance of four paradigms under majority voting (4, 8, 16, and 32 rounds). Inference time was measured by the average number of output tokens per problem. Although Qwen2.5-72B-Vanilla shows a steady increase in performance with majority voting, the improvement is minimal, with accuracy rising only from 74.31% to 74.63%. Interestingly, when majority voting is combined with CoT reasoning (Qwen2.5-72B-Vanilla CoT), more improvements are observed. However, the accuracy reaches a peak of 80.44% at higher token counts before slightly declining to 79.81%. **Marginal gains of applying majority voting** are also observed in the proposed journey learning schemes (i.e., LongStep and LongMonolog), but more obvious than that in previous methods. Qwen2.5-72B-LongStep benefits a 1.26% increment from majority voting while LongMonolog benefits 1.50%. These results indicate that while majority voting can help refine predictions by aggregating outputs from multiple runs, it does not significantly enhance performance in tasks when intermediate steps are unthoughtful to achieve consistency in voting. Journey learning, which includes nuanced thoughts for reasoning, is a more hopeful way to enhance performance via majority voting.

As we stated at the beginning of this section, we only select models benefiting from vanilla CoT for further exploration. There is a question: **Does inference-time scaling always help?** From this starting point, we first lay out the benefits of models using CoT prompting to solve medical problems of various difficulties. As vividly depicted in Figure 4, the models possessing a huge number of parameters are those achieving positive gains from CoT prompting. For models with smaller parameter sizes, such as 7B or 20B, increased inference time can unfortunately lead to performance degradation and, at times, failure to adhere to the instructed output format. On datasets of higher difficulty like JAMA, which contain challenging real-world clinical cases and require extensive domain knowledge for analysis, the performance deficits are particularly pronounced. Another noteworthy observation is that models with fewer parameters, such as Qwen2.5-32B and Qwen-72B respectively achieve increments of +1.66% / +3.28% (vanilla CoT), +2.93% / +5.12% (CoT), +5.88% / +9.69% (LongStep) and +6.03% / +11.36% (LongMonolog). Based on these findings, the underlying philosophy we hypothesize is: **The functioning of long thought during**

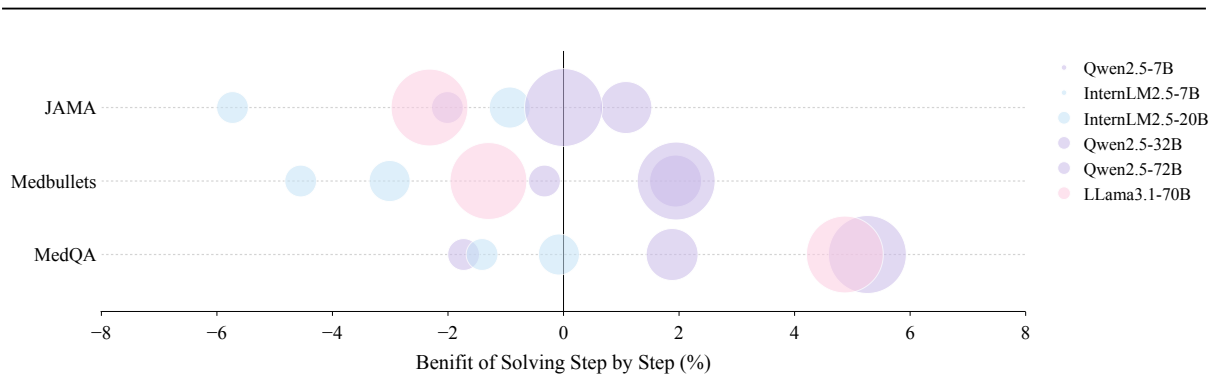


Figure 4: The benefits of prompting open-source models to solve problems step by step are illustrated. The positive axis indicates that breaking down the problem into smaller steps can enhance model performance, while the negative axis suggests that doing so may lead to diminished returns. Each bubble represents a different model, with bubble size corresponding to the model’s parameter size.

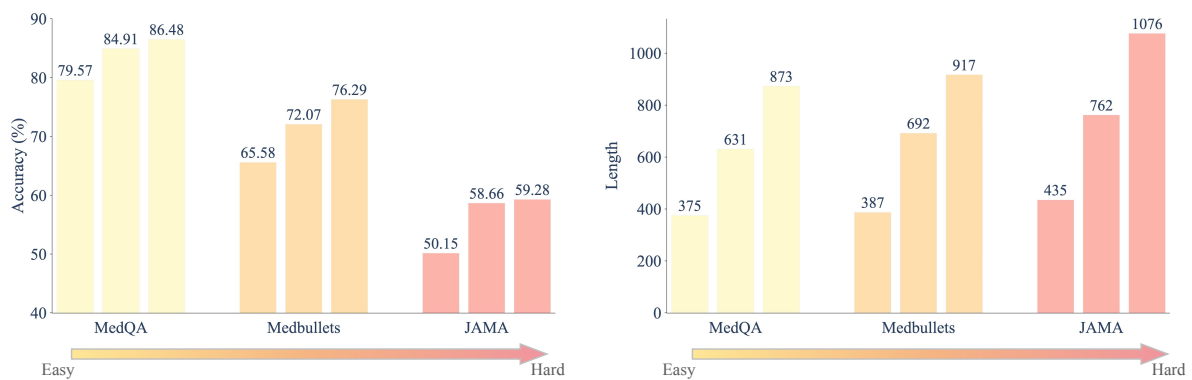


Figure 5: Comparison of accuracy and average length of output tokens of Qwen2.5-72B across three datasets using distinct strategies(from left to right: Vanilla CoT, LongStep and LongMonolog)

inference time requires sufficient capability, otherwise a futile effort is expected. This is particularly significant in medicine, where solving clinical problems depends on the capacity to understand and generate complex and nuanced text and extensive knowledge, including aspects of diseases, pharmacology, and treatment protocols.

3.4 Harder Tasks, Longer Thoughts, More Inference Time

The right part of Figure 5 reveals an intriguing observation: harder tasks appear to require longer output tokens to benefit from inference-time computing. To contextualize the level of difficulty, we hypothesized that answering questions in JAMA is more challenging than in Medbullets and MedQA, as JAMA presents more comprehensive real-world scenarios, and even proprietary models do not work well on JAMA. Additionally, we posited that Medbullets is more difficult than MedQA, as MedQA partially includes *Step 1* questions from the USMLE. This hypothesis is partially validated by the overall performance of various settings presented on the left of Figure 5, where MedQA achieves the highest accuracy, followed by Medbullets and JAMA.

Examining the length of output tokens, Qwen2.5-72B utilizes an average of 1,076 tokens to answer questions in JAMA through detailed monolog, compared to 917 tokens in Medbullets and 873 tokens in MedQA. A similar increase in output length with task difficulty is evident across other reasoning paradigms and base models, as depicted in Table 1. This philosophy is consistent with our initial observations outlined in Section 2, higher-difficulty questions necessitate more reasoning steps, thereby requiring more complex thinking and longer output during inference.

Another interesting observation is that models with fewer parameters, such as Qwen2.5-32B, tend to generate longer outputs when thinking aloud, particularly for easier questions. However, the opposite trend is observed in the other two reasoning paradigms, vanilla CoT prompting and long monolog SFT. Weaker models produce shorter responses in the former and outputs of similar length in the latter. After reviewing some examples, this discrepancy may stem from unnecessary verbosity when generating long monolog, as illustrated in Figures 10, 13 and 14.⁸ A weaker model may overlook or misinterpret key points during a long monolog, becoming stuck in confusion

⁸<https://jamanetwork.com/journals/jamadermatology/fullarticle/2797659>

or arriving at incorrect conclusions. This finding, from the other side, supports the previous hypothesis that the functioning of inference-time scaling should be based on adequate knowledge.

3.5 Generalizability and Future Directions

When we take a closer look at the curated data in LongStep (in Figure 11) and LongMonolog dataset (in Figure 12), a surprising finding is that the data are not bounded by the options provided. The a priori options as input are internalized as heuristics for developing the output thought during inference time, which more resembles a complete diagnosis with differential candidates (and exclusion of them), rather than discussing the options sequentially. To verify whether models trained on journey learning data can be effective in the differential diagnosis context, we conducted a preliminary study. We removed the multiple-choice options and allowed the model to respond freely. To ensure fairness, we selected cases published in the 2024 JAMA Clinical Challenges while the training data were collected before October 2023. It is important to note that our model was exclusively trained on journey learning data, where the synthesis process included the provision of multiple-choice options. Figures 6 to 8⁹ presents a representative case demonstrating the application of long-form reasoning for diagnosis. With long-form reasoning, the model tends to analyze a broader range of potential diseases while integrating various contextual information and its knowledge to approach more and more concise conclusions. These results offer promising insights for future research directions.

4 Conclusion

Building upon our initial exploration of inference-time scaling in the medical domain, our findings indicate that this approach offers promising enhancements for tackling complex reasoning tasks. This study demonstrated that *inference-time scaling* significantly improves model performance across benchmarks like MedQA, Medbullets, and JAMA Clinical Challenges, with accuracy gains of 6–11% achieved using only 500 training samples. Key insights at this stage primarily concern the effectiveness of scaling inference time. While majority voting offers a straightforward method to enhance inference-time computation, its impact remains limited compared to long reasoning paradigms. The necessity of extended reasoning for harder tasks underscores the scalability of inference-time scaling with task complexity. Furthermore, the shift from multiple-choice formats to free-form responses revealed the potential for nuanced medical journey learning, fostering deeper clinical reasoning capabilities.

Through continued exploration and iterative improvements, we aim to enhance the interpretability and effectiveness of inference-time scaling for addressing real-world medical challenges. By focusing on collaborative research and open resource sharing, we aim to strengthen the connection between computational advancements and real-world medical applications, ultimately improving diagnostic accuracy, patient outcomes, and healthcare efficiency. Our long-term goal is to develop intelligent systems that complement clinical expertise and address the growing complexity of modern medicine.

Case: Problem of Differential Diagnosis

A 72-year-old man with a history of polycythemia vera (positive for JAK2 V617F) presented with several months of functional decline and weight loss. Previous imaging obtained a year prior showed hepatomegaly (18 cm) and mild perinephric stranding bilaterally. On admission, physical examination findings revealed tense ascites without telangiectasia, jaundice, or other skin changes. Initial workup showed macrocytic anemia (hemoglobin, 11.8 g/dL [to convert to g/L, multiply by 10]; mean corpuscular volume, 106 μm^3), thrombocytopenia ($88 \times 10^3 \mu\text{L}$), normal white blood cell count ($5.19 \times 10^3 \mu\text{L}$ [to convert to $\times 10^9 \text{L}^{-1}$, multiply by 0.001]) with lymphopenia ($0.72 \times 10^3 \mu\text{L}$ [to convert to $\times 10^9 \text{L}^{-1}$, multiply by 0.001]), hypoalbuminemia (2.2 g/dL [to convert to g/L, multiply by 10]), elevated alkaline phosphatase (655 U/L; reference, 41–133 U/L [to convert to $\mu\text{kat/L}$, multiply by 0.0167]), and hyperbilirubinemia (total, 2.1 mg/dL; reference, 0.3–1.2; direct, 1.3 mg/dL [to convert to $\mu\text{mol/L}$, multiply by 17.104]) with otherwise normal levels of creatinine, alanine aminotransferase, and aspartate aminotransferase. Findings of activated partial thromboplastin time and international normalized ratio were also normal, and there was no significant proteinuria. An 18F-fluorodeoxyglucose (FDG) positron emission tomography/computed tomography showed soft tissue infiltrates and sclerosis of the perirenal spaces with FDG uptake, hepatosplenomegaly, ascites, and FDG avid sclerotic lesions throughout the pelvis, lumbosacral spine, and bilateral femurs. Several abdominopelvic FDG avid lymph nodes were also seen. Perinephric fibrosis and hepatomegaly were significantly worse compared with previous imaging obtained 12 months prior. A, 18F-fluorodeoxyglucose (FDG) positron emission tomography (PET)/computed tomography (CT) showing FDG uptake in the perirenal space (white arrowheads) and sclerotic bone lesions with FDG uptake (yellow arrowheads). B, Abdomen CT showing perirenal fibrosis (arrowheads) and sclerotic bone lesions in the sacrum. What is your diagnosis?

Figure 6: Problem of Differential Diagnosis from JAMA Clinical Challenges

⁹<https://jamanetwork.com/journals/jamaoncology/fullarticle/2825256>

Case: Output of Qwen2.5-72B to Differential Diagnosis (X)

The patient's clinical presentation and imaging findings suggest a complex and evolving condition that is likely related to his underlying polycythemia vera (PV). Here's a step-by-step analysis of the key points:

1. **Clinical History and Symptoms:**

- **Age and Gender:** 72-year-old male.
- **Underlying Condition:** Polycythemia vera (JAK2 V617F positive).
- **Symptoms:** Functional decline and weight loss over several months.
- **Physical Examination:** Tense ascites, no telangiectasia, jaundice, or other skin changes.

2. **Laboratory Findings:**

- **Hematologic Parameters:**
 - Macrocytic anemia (Hemoglobin 11.8 g/dL, MCV 106 μm^3).
 - Thrombocytopenia ($88 \times 10^3/\mu\text{L}$).
 - Normal white blood cell count ($5.19 \times 10^3/\mu\text{L}$) with lymphopenia ($0.72 \times 10^3/\mu\text{L}$).
- **Biochemical Parameters:**
 - Hypoalbuminemia (2.2 g/dL).
 - Elevated alkaline phosphatase (655 U/L).
 - Hyperbilirubinemia (Total 2.1 mg/dL, Direct 1.3 mg/dL).
 - Normal creatinine, ALT, and AST.
 - Normal coagulation parameters (aPTT and INR).

3. **Imaging Findings:**

- **Previous Imaging (1 year ago):**
 - Hepatomegaly (18 cm).
 - Mild perinephric stranding bilaterally.
- **Current Imaging (18F-FDG PET/CT):**
 - Soft tissue infiltrates and sclerosis of the perirenal spaces with FDG uptake.
 - Hepatosplenomegaly.
 - Ascites.
 - FDG-avid sclerotic lesions throughout the pelvis, lumbosacral spine, and bilateral femurs.
 - FDG-avid lymph nodes in the abdominopelvic region.
 - Significant worsening of perinephric fibrosis and hepatomegaly compared to previous imaging.

4. **Differential Diagnosis:**

- **Transformation of PV to Myelofibrosis:** Given the patient's history of PV and the presence of splenomegaly, hepatomegaly, and bone marrow fibrosis (sclerotic lesions), this is a strong possibility. The FDG uptake in these areas suggests active disease.
- **Secondary Amyloidosis:** This can occur in chronic myeloproliferative disorders and can present with organomegaly, hypoalbuminemia, and ascites.
- **Malignancy:** The presence of FDG-avid lymph nodes and bone lesions raises the possibility of a secondary malignancy, such as lymphoma or metastatic disease.

5. **Conclusion:**

- The most likely diagnosis is **transformation of polycythemia vera to myelofibrosis**. This is supported by the clinical symptoms, laboratory findings (anemia, thrombocytopenia, hypoalbuminemia, and elevated alkaline phosphatase), and imaging findings (hepatosplenomegaly, perinephric fibrosis, and FDG-avid sclerotic bone lesions).

Therefore, the diagnosis is: **Transformation of Polycythemia Vera to Myelofibrosis**.

Figure 7: Free-form Response: Incorrect Output of Qwen2.5-72B to Differential Diagnosis

Case: Output of Qwen2.5-72B-LongMonolog to Differential Diagnosis (✓)

##Process

Alright, let's dive into this case. A 72-year-old man with a history of polycythemia vera (PV), positive for JAK2 V617F mutation, presents with several months of functional decline and weight loss. Hmm, functional decline and weight loss in an elderly patient—immediately raises concerns about systemic illness or malignancy.

Looking back, previous imaging from a year ago showed hepatomegaly (18 cm) and mild perinephric stranding bilaterally. Now, on admission, he has tense ascites without telangiectasia, jaundice, or other skin changes. So, his liver and spleen might be enlarged, and he's retaining fluid.

His labs show macrocytic anemia (hemoglobin 11.8 g/dL, MCV 106 μm^3), thrombocytopenia (platelets $88 \times 10^3/\mu\text{L}$), normal white blood cell count but with lymphopenia ($0.72 \times 10^3/\mu\text{L}$). He also has hypoalbuminemia (2.2 g/dL), elevated alkaline phosphatase (655 U/L), and hyperbilirubinemia (total bilirubin 2.1 mg/dL, direct 1.3 mg/dL). Creatinine, AST, and ALT are normal, and no significant proteinuria.

The FDG-PET/CT shows soft tissue infiltrates and sclerosis of the perirenal spaces with FDG uptake, hepatosplenomegaly, ascites, and FDG-avid sclerotic lesions throughout the pelvis, lumbosacral spine, and bilateral femurs. There are also FDG-avid lymph nodes in the abdomen and pelvis. Perinephric fibrosis and hepatomegaly are worse than a year ago.

So, what could be going on here?

Firstly, his PV is known, which is a myeloproliferative neoplasm (MPN). Over time, MPNs can transform into more aggressive diseases. Possible complications include myelofibrosis, acute leukemia, or even extramedullary hematopoiesis. Wait, the FDG-avid sclerotic bone lesions and lymphadenopathy suggest active cell turnover or malignancy. The perirenal fibrosis and soft tissue infiltrates with FDG uptake point toward infiltration by malignant cells.

Could this be acute myeloid leukemia (AML)? AML can arise from MPNs, but typically we'd see a high peripheral blast count, which doesn't seem to be the case here—the WBC count is normal.

What about myelofibrosis? Myelofibrosis is a known complication of PV where fibrosis replaces normal bone marrow, leading to extramedullary hematopoiesis in organs like the liver and spleen. Symptoms include splenomegaly, constitutional symptoms, and cytopenias due to ineffective hematopoiesis.

But would myelofibrosis explain the sclerotic bone lesions and FDG-avid lymph nodes? Usually, myelofibrosis leads to bone pain and osteosclerosis, but I'm not sure if it causes FDG-avid lesions.

Alternatively, could this be a secondary amyloidosis? Amyloidosis can result from chronic inflammation or malignancy and leads to organ deposition of amyloid proteins. It can cause organomegaly, macroglossia, skin changes, and involvement of the kidneys and heart. However, our patient doesn't have these features.

Hmm, maybe Castleman disease? It's a lymphoproliferative disorder that can cause systemic symptoms and lymphadenopathy. But Castleman disease doesn't typically cause sclerotic bone lesions or perirenal fibrosis.

Wait, could this be light-chain deposition disease or multiple myeloma? Multiple myeloma is a plasma cell malignancy causing bone lesions, often sclerotic or lytic, and can lead to renal issues. But patients usually present with anemia, hypercalcemia, and elevated immunoglobulins, which don't seem prominent here.

Perhaps it's POEMS syndrome? Polyneuropathy, Organomegaly, Endocrinopathy, Monoclonal gammopathy, and Skin changes. Our patient has hepatomegaly and sclerotic bone lesions, but there's no mention of neuropathy, endocrine issues, or skin changes.

Hold on, the perirenal fibrosis and sclerotic lesions make me think of Erdheim-Chester disease (ECD). ECD is a rare non-Langerhans histiocytosis characterized by the proliferation of histiocytes leading to fibrosis and infiltration of various organs.

ECD commonly affects middle-aged adults and involves the bones, especially the long bones and axial skeleton, causing sclerotic lesions. It also frequently affects the central nervous system, lungs, and skin. Perirenal fibrosis is a hallmark of ECD and can lead to hypertension and renal dysfunction.

Additionally, ECD can involve the skin, CNS, orbits, and other organs. Patients often present with diabetes insipidus, pulmonary symptoms, and neurological signs. Our patient doesn't have these symptoms, but perhaps they haven't developed yet.

Also, ECD is often associated with BRAF V600E mutations or MAPK pathway alterations. However, it can coexist with MPNs like PV, which have JAK2 mutations.

Wait, could the JAK2 V617F mutation in PV somehow be related to ECD? While they involve different signaling pathways, both conditions involve dysregulated cell proliferation.

Alternatively, could this be extramedullary hematopoiesis? In advanced myelofibrosis, the body compensates for bone marrow failure by producing blood cells in the spleen, liver, and other organs. This can cause organomegaly and fibrosis. But extramedullary hematopoiesis wouldn't explain the sclerotic bone lesions or FDG-avid lymph nodes.

Maybe I'm missing something. Let's revisit myelofibrosis. Secondary myelofibrosis from PV can cause bone pain, splenomegaly, and extramedullary hematopoiesis. The fibrosis could lead to sclerotic bone lesions.

But would it cause perirenal fibrosis? Well, fibrosis is a common theme.

Also, the elevated alkaline phosphatase suggests active bone turnover, supporting bone involvement.

Given all this, I think myelofibrosis is a strong possibility.

However, considering the perirenal fibrosis and sclerotic lesions, ECD remains a compelling diagnosis.

Wait, perhaps a combination of both? Could the PV have transformed into myelofibrosis, and concurrently, ECD has developed?

Alternatively, perhaps the histiocyte proliferation in ECD is mimicking myelofibrosis.

Given the rarity of ECD and the presence of hallmark features like perirenal fibrosis and sclerotic bone lesions, I think ECD is the most likely diagnosis.

Therefore, after considering all possibilities, I believe the diagnosis is **Erdheim-Chester disease**.

Figure 8: Free-form Resposns: Correct Output of Qwen2.5-72B-LongMonolog to Differential Diagnosis

References

- [1] AI@Meta. 2024. [Llama 3 model card](#).
- [2] Tom Brown, Benjamin Mann, Nick Ryder, Melanie Subbiah, Jared D Kaplan, Prafulla Dhariwal, Arvind Neelakantan, Pranav Shyam, Girish Sastry, Amanda Askell, et al. 2020. Language models are few-shot learners. *Advances in neural information processing systems*, 33:1877–1901.
- [3] Hanjie Chen, Zhouxiang Fang, Yash Singla, and Mark Dredze. 2024. Benchmarking large language models on answering and explaining challenging medical questions. *arXiv preprint arXiv:2402.18060*.
- [4] Aakanksha Chowdhery, Sharan Narang, Jacob Devlin, Maarten Bosma, Gaurav Mishra, Adam Roberts, Paul Barham, Hyung Won Chung, Charles Sutton, Sebastian Gehrmann, et al. 2023. Palm: Scaling language modeling with pathways. *Journal of Machine Learning Research*, 24(240):1–113.
- [5] Suriya Gunasekar, Yi Zhang, Jyoti Aneja, Caio César Teodoro Mendes, Allie Del Giorno, Sivakanth Gopi, Mojan Javaheripi, Piero Kauffmann, Gustavo de Rosa, Olli Saarikivi, et al. 2023. Textbooks are all you need. *arXiv preprint arXiv:2306.11644*.
- [6] Geoffrey Hinton. 2015. Distilling the knowledge in a neural network. *arXiv preprint arXiv:1503.02531*.
- [7] Edward J Hu, Yelong Shen, Phillip Wallis, Zeyuan Allen-Zhu, Yuanzhi Li, Shean Wang, Lu Wang, and Weizhu Chen. 2021. Lora: Low-rank adaptation of large language models. *arXiv preprint arXiv:2106.09685*.
- [8] Zhen Huang, Haoyang Zou, Xuefeng Li, Yixiu Liu, Yuxiang Zheng, Ethan Chern, Shijie Xia, Yiwei Qin, Weizhe Yuan, and Pengfei Liu. 2024. O1 replication journey—part 2: Surpassing o1-preview through simple distillation, big progress or bitter lesson? *arXiv preprint arXiv:2411.16489*.
- [9] Jinhao Jiang, Zhipeng Chen, Yingqian Min, Jie Chen, Xiaoxue Cheng, Jiapeng Wang, Yiru Tang, Haoxiang Sun, Jia Deng, Wayne Xin Zhao, et al. 2024. Technical report: Enhancing llm reasoning with reward-guided tree search. *CoRR*, abs/2411.11694.
- [10] Di Jin, Eileen Pan, Nassim Oufattole, Wei-Hung Weng, Hanyi Fang, and Peter Szolovits. 2020. What disease does this patient have? a large-scale open domain question answering dataset from medical exams. *arXiv preprint arXiv:2009.13081*.
- [11] Jared Kaplan, Sam McCandlish, Tom Henighan, Tom B Brown, Benjamin Chess, Rewon Child, Scott Gray, Alec Radford, Jeffrey Wu, and Dario Amodei. 2020. Scaling laws for neural language models. *arXiv preprint arXiv:2001.08361*.
- [12] Kimi. 2024. [k0math](#).
- [13] OpenAI. 2024. [Learning to reason with llms](#).
- [14] Yiwei Qin, Xuefeng Li, Haoyang Zou, Yixiu Liu, Shijie Xia, Zhen Huang, Yixin Ye, Weizhe Yuan, Hector Liu, Yuanzhi Li, and Pengfei Liu. 2024. [O1 replication journey: A strategic progress report – part 1](#). *CoRR*.
- [15] Pengcheng Qiu, Chaoyi Wu, Xiaoman Zhang, Weixiong Lin, Haicheng Wang, Ya Zhang, Yanfeng Wang, and Weidi Xie. 2024. Towards building multilingual language model for medicine. *Nature Communications*, 15(1):8384.
- [16] Jeff Rasley, Samyam Rajbhandari, Olatunji Ruwase, and Yuxiong He. 2020. Deepspeed: System optimizations enable training deep learning models with over 100 billion parameters. In *Proceedings of the 26th ACM SIGKDD International Conference on Knowledge Discovery & Data Mining*, pages 3505–3506.
- [17] Robert H Seller and Andrew B Symons. 2011. *Differential Diagnosis of Common Complaints E-Book*. Elsevier Health Sciences.
- [18] Karan Singhal, Shekoofeh Azizi, Tao Tu, S Sara Mahdavi, Jason Wei, Hyung Won Chung, Nathan Scales, Ajay Tanwani, Heather Cole-Lewis, Stephen Pfohl, et al. 2023. Large language models encode clinical knowledge. *Nature*, 620(7972):172–180.
- [19] Charlie Snell, Jaehoon Lee, Kelvin Xu, and Aviral Kumar. 2024. Scaling llm test-time compute optimally can be more effective than scaling model parameters. *arXiv preprint arXiv:2408.03314*.
- [20] Rohan Taori, Ishaan Gulrajani, Tianyi Zhang, Yann Dubois, Xuechen Li, Carlos Guestrin, Percy Liang, and Tatsunori B Hashimoto. 2023. Alpaca: A strong, replicable instruction-following model. *Stanford Center for Research on Foundation Models*. <https://crfm.stanford.edu/2023/03/13/alpaca.html>, 3(6):7.
- [21] Qwen Team. 2024a. [Qwen2.5: A party of foundation models](#).

-
- [22] Qwen Team. 2024b. Qwq: Reflect deeply on the boundaries of the unknown.
- [23] Skywork o1 Team. 2024. Skywork-o1 open series. <https://huggingface.co/Skywork>.
- [24] Jason Wei, Xuezhi Wang, Dale Schuurmans, Maarten Bosma, Fei Xia, Ed Chi, Quoc V Le, Denny Zhou, et al. 2022. Chain-of-thought prompting elicits reasoning in large language models. *Advances in neural information processing systems*, 35:24824–24837.
- [25] Can Xu, Qingfeng Sun, Kai Zheng, Xiubo Geng, Pu Zhao, Jiazhan Feng, Chongyang Tao, and Daxin Jiang. 2023. Wizardlm: Empowering large language models to follow complex instructions. *arXiv preprint arXiv:2304.12244*.
- [26] Di Zhang, Jianbo Wu, Jingdi Lei, Tong Che, Jiatong Li, Tong Xie, Xiaoshui Huang, Shufei Zhang, Marco Pavone, Yuqiang Li, Wanli Ouyang, and Dongzhan Zhou. 2024a. Llama-berry: Pairwise optimization for o1-like olympiad-level mathematical reasoning. *CoRR*, abs/2410.02884.
- [27] Yuxiang Zhang, Shangxi Wu, Yuqi Yang, Jiangming Shu, Jinlin Xiao, Chao Kong, and Jitao Sang. 2024b. o1-coder: an o1 replication for coding. *CoRR*, abs/2412.00154.
- [28] Yaowei Zheng, Richong Zhang, Junhao Zhang, Yanhan Ye, Zheyang Luo, Zhangchi Feng, and Yongqiang Ma. 2024. Llamafactory: Unified efficient fine-tuning of 100+ language models. *arXiv preprint arXiv:2403.13372*.

A Appendix

Case: Problem

A 68-year-old man comes to the physician because of recurrent episodes of nausea and abdominal discomfort for the past 4 months. The discomfort is located in the upper abdomen and sometimes occurs after eating, especially after a big meal. He has tried to go for a walk after dinner to help with digestion, but his complaints have only increased. For the past 3 weeks he has also had symptoms while climbing the stairs to his apartment. He has type 2 diabetes mellitus, hypertension, and stage 2 peripheral arterial disease. He has smoked one pack of cigarettes daily for the past 45 years. He drinks one to two beers daily and occasionally more on weekends. His current medications include metformin, enalapril, and aspirin. He is 168 cm (5 ft 6 in) tall and weighs 126 kg (278 lb); BMI is 45 kg/m². His temperature is 36.4 ° C (97.5 ° F), pulse is 78/min, and blood pressure is 148/86 mm Hg. On physical examination, the abdomen is soft and nontender with no organomegaly. Foot pulses are absent bilaterally. An ECG shows no abnormalities. Which of the following is the most appropriate next step in diagnosis?

A: Esophagogastroduodenoscopy B: Hydrogen breath test
C: Cardiac stress test D: Abdominal ultrasonography of the right upper quadrant

Figure 9: Case of problems for synthesizing data.

Case: Problem

A man in his 80s with a medical history of gastric adenocarcinoma treated with total gastrectomy presented with asymptomatic lesions on his tongue that gradually developed during the previous 3 months. Intraoral examination revealed multiple yellowish to erythematous papules and verrucous cobblestone-like plaques on the mucosal surface on both sides of his tongue (Figure, A and B). The skin of the face, neck, arms, and other sun-exposed areas did not reveal any associated lesions. He reported occasional alcohol intake, and there was no history of tobacco-related habits or oral trauma. The results of laboratory investigations, including a complete blood cell count, serum chemistry panel, liver and kidney function test, C-reactive protein levels, lipid profile, and serum and urine electrophoresis disclosed no abnormalities. With the clinical suspicion of squamous cell carcinoma, an incisional biopsy was performed (Figure, C and D). Yellowish plaques in a cobblestone pattern on the right (A) and left (B) side of the tongue. C and D, Circumscribed eosinophilic, amorphous fissured masses in the subepithelial connective tissue (hematoxylin-eosin). What Is Your Diagnosis?

A: Verrucous xanthoma B: Colloid milium—classic adult type
C: Nodular amyloidosis D: Nodular colloid degeneration

Figure 10: One case of JAMA problems.

Case: Distilled Long Step to The Problem

To solve this problem step by step, let's analyze the patient's presentation, risk factors, and the most appropriate next diagnostic step.

****Patient Presentation and History:****

- ****Age:**** 68-year-old man.
- ****Symptoms:****
 - Recurrent episodes of ****nausea and upper abdominal discomfort**** for the past 4 months.
 - Discomfort occurs ****after eating****, especially large meals.
 - ****Increased discomfort with walking after dinner****.
 - For the past 3 weeks, ****symptoms occur while climbing stairs****.
- ****Medical History:****
.....
- ****Lifestyle Factors:****
.....
- ****Medications:****
.....
- ****Physical Exam:****
.....
- ****Investigations:****
 - ****ECG shows no abnormalities****.

****Analysis:****

1. ****Risk Factors for Cardiovascular Disease:****

- ****Age**** (68 years old).
- ****Gender**** (male).
- ****Smoking history**** (45 pack-years).
- ****Hypertension****.
- ****Type 2 diabetes mellitus****.
- ****Peripheral arterial disease****.
- ****Obesity**** (BMI of 45 kg/m²).

2. ****Symptoms Suggestive of Cardiac Ischemia:****

- ****Exertional symptoms:**** Discomfort increases with physical activity (walking after meals, climbing stairs).
- ****Atypical presentation:**** In diabetics, myocardial ischemia can present atypically, sometimes as gastrointestinal discomfort.

3. ****Differential Diagnosis:****

- ****Cardiac ischemia (angina pectoris):**** Likely given the risk factors and exertional nature of symptoms.
- ****Gastrointestinal causes:****
 - ****Peptic ulcer disease/gastritis:**** Less likely without epigastric tenderness or specific GI findings.
 - ****Gallstones (cholelithiasis):**** Would present with right upper quadrant pain, not necessarily exertional.
 - ****Gastroparesis:**** Common in diabetics but doesn't explain exertional symptoms.
 - ****Mesenteric ischemia:**** Chronic mesenteric ischemia causes postprandial pain but is less likely to be exertional.

4. ****Investigations to Consider:****

- ****Cardiac stress test:**** To evaluate for ischemia during exertion.
- ****Esophagogastroduodenoscopy (EGD):**** To examine for GI causes like ulcers or gastritis.
- ****Hydrogen breath test:**** For lactose intolerance or bacterial overgrowth (less likely given symptoms).
- ****Abdominal ultrasonography:**** To assess gallbladder; less likely given the absent right upper quadrant tenderness.

****Conclusion:****

Given the patient's risk factors and symptoms that worsen with exertion, cardiac ischemia is the most probable cause. A normal ECG does not rule out ischemia, especially in diabetics who may have silent or atypical presentations. Therefore, the most appropriate next step is to perform a ****cardiac stress test**** to evaluate for exertional myocardial ischemia.

****Answer is: (C: Cardiac stress test)****

Figure 11: Case of our distilled long step data for the problem.

Case: Distilled Long Monolog to The Problem

Process

Alright, let's take a closer look at this patient. He's a 68-year-old man with recurrent episodes of nausea and upper abdominal discomfort for the past four months. The discomfort occurs after eating, especially large meals, and has increased when he goes for a walk after dinner. Interestingly, he's also started experiencing symptoms while climbing the stairs to his apartment over the past three weeks.

He has a significant medical history: type 2 diabetes mellitus, hypertension, stage 2 peripheral arterial disease. He smokes a pack of cigarettes daily and has been doing so for 45 years. His BMI is quite high at 45 kg/m², indicating obesity. On examination, his abdomen is soft and nontender, and foot pulses are absent bilaterally. His ECG is normal.

First, I need to consider what could be causing his symptoms. Upper abdominal discomfort and nausea after eating large meals could suggest gastrointestinal issues like gastroesophageal reflux disease (GERD), peptic ulcer disease, or even gallstones. Maybe an esophagogastroduodenoscopy (EGD) or an abdominal ultrasound could be helpful.

But wait, he also experiences symptoms when walking after dinner and while climbing stairs. That suggests that his symptoms are not just related to eating but also to exertion. Could this be angina presenting atypically?

Given his extensive cardiovascular risk factors—age, hypertension, diabetes, smoking, obesity, peripheral arterial disease—coronary artery disease (CAD) is a strong possibility. Angina can sometimes present as abdominal discomfort, especially in older patients or those with diabetes, who might have atypical presentations due to autonomic neuropathy.

Also, the fact that his foot pulses are absent bilaterally indicates significant peripheral arterial disease, which often coexists with coronary artery disease. His normal ECG doesn't rule out ischemia, especially if he's not currently experiencing symptoms during the ECG.

Now, considering the gastrointestinal possibilities: GERD or peptic ulcer disease could cause postprandial discomfort, but they are less likely to cause symptoms with exertion. Gallstones could cause right upper quadrant pain, and an abdominal ultrasound would be useful there, but his pain is in the upper abdomen generally, not specifically the right upper quadrant, and there's no mention of jaundice or other biliary symptoms.

A hydrogen breath test would help diagnose small intestinal bacterial overgrowth or lactose intolerance, but these typically cause bloating, gas, and diarrhea, which aren't mentioned here.

So, the most logical step is to assess for coronary artery disease. A cardiac stress test would help evaluate for ischemia that's brought on by exertion or increased metabolic demand after eating a large meal.

I almost made the mistake of focusing on gastrointestinal causes because of the postprandial nature of his symptoms. But the exertional component and his cardiovascular risk factors point more towards cardiac ischemia.

Therefore, the most appropriate next step in diagnosis is a cardiac stress test.

Correct option

****C: Cardiac stress test****

Figure 12: One case of our distilled long Monolog data for the problem.

Case: Long Step to The Problem

To solve this problem step by step, we'll analyze the patient's presentation, histopathological findings, and compare them with the options provided.

****Patient Presentation:****

- ****Age:**** Man in his 80s.
- ****Medical History:**** Gastric adenocarcinoma treated with total gastrectomy.
- ****Symptoms:**** Asymptomatic lesions on the tongue developing over 3 months.
- ****Clinical Findings:**** Multiple yellowish to erythematous papules and verrucous cobblestone-like plaques on the tongue mucosa.
- ****Examination Elsewhere:**** No associated lesions on sun-exposed skin.
- ****Lifestyle:**** Occasional alcohol intake; no tobacco use or oral trauma.
- ****Laboratory Investigations:**** Normal complete blood count, serum chemistry, liver and kidney function tests, C-reactive protein levels, lipid profile, and serum/urine electrophoresis.
- ****Histopathology:**** Circumscribed eosinophilic, amorphous, fissured masses in the subepithelial connective tissue.

****Analysis of Options:****

****Option A: Verrucous Xanthoma****

- ****Typical Features:**** Presents as solitary or multiple yellowish papules or nodules on the oral mucosa, often associated with xanthelasma.
- ****Histopathology:**** Lipid-laden macrophages (foam cells) in the dermis.
- ****Relevance:**** While it can present with verrucous lesions, the histopathology doesn't match the eosinophilic, amorphous masses described.

****Option B: Colloid Milium–Classic Adult Type****

- ****Typical Features:**** Presents as translucent, firm, dome-shaped papules on sun-exposed areas (face, neck).
- ****Histopathology:**** Amorphous eosinophilic material in the dermis, representing hyalinized collagen.
- ****Relevance:**** Lesions are typically on sun-exposed skin, not the oral mucosa, and the patient has no such lesions.

****Option C: Nodular Amyloidosis****

- ****Typical Features:**** Presents as solitary or multiple nodules in various locations, including the tongue.
- ****Histopathology:**** Congo red-positive amyloid deposits with apple-green birefringence under polarized light.
- ****Relevance:**** Amyloid deposits appear as eosinophilic, amorphous material but require special staining for diagnosis.

****Option D: Nodular Colloid Degeneration****

- ****Typical Features:**** Presents as nodular lesions on the tongue, especially in elderly patients.
- ****Histopathology:**** Eosinophilic, amorphous, fissured masses in the subepithelial connective tissue.
- ****Relevance:**** Matches the clinical presentation and histopathological findings described.

****Conclusion:****

Given the patient's age, the location of lesions on the tongue, the absence of lesions on sun-exposed skin, and the histopathological description of eosinophilic, amorphous, fissured masses in the subepithelial connective tissue, the most likely diagnosis is ****Nodular Colloid Degeneration****.

****Answer is: (D: Nodular colloid degeneration)****



Figure 13: Generated Thought by the Qwen2.5-32B-LongStep Model.

Case: Long Monolog to The Problem

Process

Alright, let's dive into this case. An elderly man in his 80s who had gastric adenocarcinoma treated with total gastrectomy is presenting with asymptomatic lesions on his tongue that have been developing over the past three months. On intraoral examination, there are multiple yellowish to erythematous papules and verrucous cobblestone-like plaques on the mucosal surface on both sides of his tongue. Importantly, there are no associated lesions on the skin of the face, neck, arms, or other sun-exposed areas. His lab results are all normal, and there's no history of tobacco use or oral trauma, though he does report occasional alcohol intake.

The biopsy shows circumscribed eosinophilic, amorphous fissured masses in the subepithelial connective tissue. They're described as "fissured," which makes me think about the microscopic appearance of certain conditions.

Now, I need to consider the options provided:

.....

First, I'll think about verrucous xanthoma. It typically presents as a single, firm, yellow nodule on the lower lip or buccal mucosa. Histologically, it shows xanthogranulomatous inflammation with Touton giant cells. But in this case, the lesions are multiple and on the tongue, not just the lower lip. Also, the biopsy mentions eosinophilic, amorphous fissured masses, which doesn't quite fit with verrucous xanthoma. So, option A seems less likely.

Next, colloid milium—classic adult type. This condition usually affects sun-exposed skin, like the face and neck, and presents as small, translucent, yellowish papules. Histologically, it shows hyaline globules in the dermis. Our patient doesn't have any lesions on sun-exposed areas, and the histology doesn't mention hyaline globules. So, option B doesn't seem to fit.

Now, nodular amyloidosis. Amyloidosis can affect various organs, including the tongue. Clinically, it might present as macroglossia or nodules on the tongue. Histologically, amyloid deposits appear as eosinophilic, amorphous material that stains positively with Congo red and shows apple-green birefringence under polarized light. The biopsy mentions eosinophilic, amorphous fissured masses, which could be consistent with amyloid deposits. Plus, the fissured appearance might correspond to the characteristic "stalactite" formation seen in amyloidosis.

Lastly, nodular colloid degeneration. This is a rare condition characterized by the deposition of hyaline material in the dermis, often associated with chronic inflammation or trauma. Histologically, it shows hyaline nodules in the dermis. However, our patient doesn't have a history of trauma, and the lesions are on the tongue, not the skin. Also, the histology mentions eosinophilic, amorphous fissured masses, not hyaline nodules.

Wait, but could I be missing something? Maybe the fissured masses in the biopsy are more characteristic of colloid degeneration? **But then again, colloid degeneration is more common in the skin and is associated with hyaline material, not eosinophilic, amorphous material.**

Also, considering the patient's history of total gastrectomy due to gastric adenocarcinoma, could there be any association with amyloidosis? Multiple myeloma and other plasma cell dyscrasias can lead to systemic amyloidosis, but there's no mention of monoclonal gammopathy or abnormal serum and urine electrophoresis. Still, the histological findings align well with amyloidosis.

I should also consider that the initial suspicion was squamous cell carcinoma, but the biopsy didn't confirm that. If it were squamous cell carcinoma, we'd expect keratin pearls and intercellular bridges, not eosinophilic, amorphous fissured masses.

So, putting it all together, nodular amyloidosis seems to be the most consistent diagnosis. The clinical presentation of multiple yellowish to erythematous papules and verrucous cobblestone-like plaques on the tongue, along with the histological finding of eosinophilic, amorphous fissured masses in the subepithelial connective tissue, points toward amyloidosis.

Therefore, I believe the correct answer is ****C: Nodular amyloidosis****.

Correct option

****C: Nodular amyloidosis****



Figure 14: Failure case generated by the Qwen2.5-32B-LongStep Model.